JOURNAL OF MATERIALS SCIENCE 25 (1990) 4815–4821

Pressureless sintering of Y_2O_3–CeO_2-doped sialons

E. SÖDERLUND, T. EKSTRÖM
Department of Inorganic Chemistry, Arrhenius Laboratory, University of Stockholm, S-106 91 Stockholm, Sweden

Various sialon materials have been prepared by pressureless sintering at 1775 and 1825° C using Y_2O_3 and/or CeO_2 as sintering aids. Constant molar amounts of the oxide mixtures were added in the ratios Y_2O_3/CeO_2: 100/0, 75/25, 50/50, 25/75, 0/100 corresponding to 6.0 and 9.25 wt% for the pure Y_2O_3 and pure CeO_2, respectively. Only one of the compositional series reached full density at 1775° C with cerium replacing yttrium, whereas at 1825° C all compositional series except one became dense. The samples sintered showed that yttrium but not cerium stabilizes the α sialon phase in these ceramics. The dense cerium–sialon ceramics sintered at 1825° C have as good hardness and indentation fracture toughness as the corresponding yttrium–sialon ceramics, or even higher for the β sialon type of materials. For the mixed α–β sialon materials the hardness decreased as the amount of α sialon phase decreased by increasing cerium-doping.

1. Introduction

The potential of silicon nitride as an engineering material was recognized about 30 years ago [1]. Silicon nitride is covalently bonded, however, and a normal sintering process to achieve dense ceramic materials, or a transformation from the α to β form the Si_3N_4 structure, will need bonds to be broken and reformed. The energy requirements of this process preclude its occurrence in the absence of a liquid or vapour medium below the decomposition temperature of about 1850° C at atmospheric pressure of nitrogen gas. The self-diffusion found in silicon nitride is extremely low, and the diffusion coefficient of nitrogen at a temperature of 1800° C is 10^{-17} and 10^{-12} cm^2 sec^{-1} in α- and β-Si_3N_4, respectively [2]. Oxide additives, therefore, promote densification because they form eutectic liquids at the sintering temperature, providing the means for liquid-phase sintering [3, 4]. If an external pressure is used, fully dense ceramic materials can be made by very small additions, i.e. by hot pressing or hot isostatic pressing. Components of silicon nitride made in the latter way have attracted much attention because of the very good properties that can be retained at high temperature, about 1300° C [5]. To make dense silicon nitride materials by pressureless sintering requires additions of much higher amounts of sintering aids, and the preparation by addition of typically 5 to 10 wt% Y_2O_3 together with 5 to 15 wt% Al_2O_3 and/or AlN to form sialon ceramics is a well established technique [6]. For sintered sialon ceramics, however, a strength reduction occurs above 900 to 1000° C and is due to the additive fluxing agents that are necessary for the densification by pressureless sintering. Upon cooling from the sintering temperature a residual glassy phase forms between the sialon grains, and the transition temperature for these yttrium sialon glasses sets the highest possible service temperature. On the other hand, at temperatures below 900 to 1000° C, the sialons offers many attractive properties, similar to the other silicon nitride-based ceramics, and they can therefore be used in different engineering applications at medium-range temperatures where most metals are insufficient.

Yttrium oxide has been used as a sintering additive to the sialon ceramics because it forms a chemically inert and refractory residual glassy phase. One drawback with yttrium oxide, and most other rare earth oxides which can be used, is the high cost level of these additives. It would, therefore, be beneficial to replace the yttrium oxide by another less expensive oxide, if the good properties found in the yttrium sialon materials are not significantly deteriorated. One interesting candidate for this purpose is cerium oxide. It is known that the Ce^{3+} ion found at high temperatures in the Ce–Si–Al–O–N system forms phases very similar to those found in the corresponding Y–Si–Al–O–N system [3, 7]. The former system is schematically illustrated as a Jänecke triangular prism in Fig. 1.

Commercially available high-purity cerium oxide CeO_2 has a cost of only one-fifth that of Y_2O_3, but metal ion is present as Ce^{4+} in this oxide. This causes no complications in pressureless sintering, however, as at a temperature well below that at which the sintering process starts, CeO_2 transforms to Ce_2O_3 by the process

$$Si_3N_4 + 12CeO_2 \rightarrow 3SiO_2 + 6Ce_2O_3 + 2N_2(g)$$

As pore closure has not occurred, the released nitrogen gas escapes from the ceramic powder compact, but one has to consider in calculating the final composition that the overall O/N ratio of the material composition will change slightly during the sintering process.

0022–2461/90 $03.00 + .12

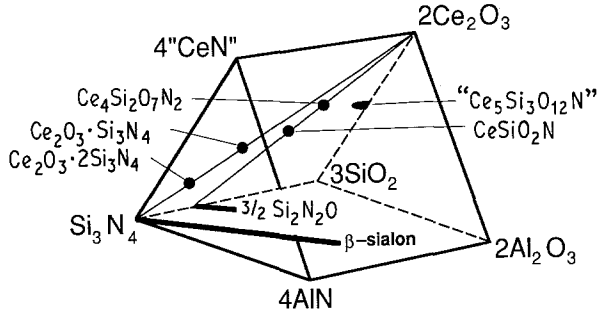

Figure 1. A part of the Ce–Si–Al–O–N system schematically drawn as a Jänecke prism. $Ce_2O_3 \cdot Si_3N_4$ is N-melilite, $CeSiO_2N$ is N-α-wollastonite, $Ce_4Si_2O_7N_2$ is called N-YAM, and "$Ce_5Si_3O_{12}N$" is N-apatite.

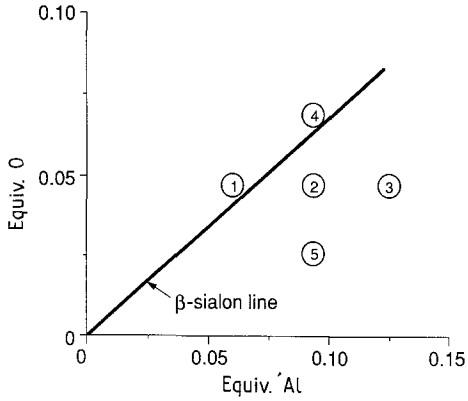

Figure 2. The overall weighted-in compositions of the samples made in this study represented as equivalents of oxygen and aluminium added to Si_3N_4. Oxygen from the added CeO_2 or Y_2O_3 is not included in the calculations of the oxygen equivalents. The reaction of CeO_2 with Si_3N_4 to form Ce_2O_3 will move the overall composition vertically by a certain amount, at most 0.006 units for pure CeO_2 additions.

In previous investigations it has been found that CeO_2 is a more effective sintering aid than Ce_2O_3, a fact which might be attributed to the "excess" of SiO_2 formed by the process described above [8, 9]. Hot-pressing of ceria-doped silicon nitride compacts at 1750° C forms fully dense materials [8, 10], and similar good results have been found by overpressure sintering (2 to 4 MPa nitrogen gas) at temperatures up to 2000° C [11–13]. It has been found more difficult, however, to obtain dense silicon nitride materials by pressureless sintering only, and in the reported investigations fairly high amounts of additives have been needed; thus, dense ceramics were obtained by 20 wt % CeO_2 [14] or by 8 wt % CeO_2 + 14 wt % SiO_2 [15]. Finally, it can be mentioned that small additions of Al_2O_3 together with CeO_2 have been observed to promote the sintering process [12].

To examine the possibilities of replacing Y_2O_3 with CeO_2 as a sintering aid in pressureless sintering, a series of M–Si–Al–O–N materials were prepared on a semi-pilot plant scale. The densification of these preparations, with evaluation of phase composition, microstructure and some mechanical properties at room temperature is reported below.

2. Experimental procedure

The selected compositions investigated in this study are shown in Fig. 2. The chosen compositions are situated close to the Si_3N_4 corner of the M–Si–Al–O–N phase diagram, comprising two samples that contain only β sialon and liquid (1, 4) and three samples (2, 3, 5) which fall in the α–β part of the Y–Si–Al–O–N system. Equivalents used in Fig. 2 are defined by the following formulae

$$\text{equiv. Al} = \frac{3(\text{at \% Al})}{3(\text{at \% Al}) + 4\,(\text{at \% Si})}$$

$$\text{equiv. O} = \frac{2(\text{at \% O})}{2(\text{at \% O}) + 3(\text{at \% N})}$$

A constant molar fraction of (Y_2O_3 + CeO_2) was added to all samples, corresponding to 6.0 and 9.25 wt % for the pure Y_2O_3 and CeO_2 specimens, respectively. The samples were prepared with mixtures of Y_2O_3/CeO_2 in the ratios 100/0, 75/25, 50/50, 25/75 and 0/100. The source materials used were silicon nitride (Starck, Berlin, grade LC1), aluminium oxide (Alcoa, Worcester, UK, grade A16SG), aluminium nitride (Starck, grade A), yttrium oxide (Starck, grade Finest) and cerium oxide (Starck, grade Finest). The analysed oxygen content of the silicon nitride corresponds to 2.9 wt % SiO_2 and the oxygen content of the aluminium nitride to 1.9 wt % Al_2O_3. The materials were synthesized on a semi-pilot plant scale with a batch size of 500 g dry weight. The starting powders were carefully weighed, taking account of the extra oxygen present on the surface of the nitride particles, and were mixed in water-free propanol and milled in a vibratory mill for 16 h with sialon milling medium. After drying, the powder mixes were dry-pressed (125 MPa) into compacts of size 16 mm × 16 mm × 6 mm. The powder compacts were embedded in a sub-micrometre BN powder bed on graphite trays and sintered at 1775 and 1825° C for 2 h in a nitrogen gas atmosphere (0.1 MPa).

Density measurements using Archimedes' principle were made with a precision of $\pm 0.002\,g\,cm^{-3}$ for any single specimen. However, the limit of accuracy obtained from series of ten different specimens of the same composition, but sintered at different positions within the furnace, was found to be about $\pm 0.01\,g\,cm^{-3}$. The sintered material was prepared for physical characterization by diamond cutting, grinding and polishing using standard techniques. Special care was taken in the final polishing step to minimize any material pull-out and to minimize any influence of compressive surface stress on subsequent physical measurements. Hardness (HV 10) and indentation fracture toughness (K_{IC}) at room temperature were obtained by a Vickers diamond indentor using a 98 N (10 kg) load, and the fracture toughness was evaluated with the method of Anstis *et al.* [16] assuming a value of 300 GPa for Young's modulus. The accuracy of repeated measurements on the same sample was ± 30 and ± 0.2 for the HV 10 and K_{IC} values, respectively.

The phase analysis was based on X-ray powder patterns recorded in a Guinier–Hägg focusing camera ($CuK\alpha_1$ radiation, silicon as internal standard). The equations $a = 0.7603 + z \cdot 0.00297$ nm and $c = 0.2907 + z \cdot 0.00255$ nm were used to calculate the z values for the β-sialon phase [17]. The errors in

the z values are within ± 0.05 units. For determining the ratio of α- to $(\alpha + \beta)$-sialon present, a simple method was used, based on the integrated intensities of the (1 0 2) and (2 1 0) reflections of the α-phase and the (1 0 1) and (2 1 0) refections of the β-phase. This method and more exact ones have been discussed recently by Käll [18]. Scanning electron microscopy was performed on carbon-coated sintered materials, using a Jeol JSM 820 instrument equipped with a Link AN 10000 EDS analyser. The chemical analysis by electron microprobe was made with a Cameca Camebax instrument.

3. Results

3.1. Density measurements

The replacement of Y_2O_3 with CeO_2 at a sintering temperature of 1775° C in general made the materials more difficult to sinter to full density, as illustrated in Fig. 3a. The only sample that became dense was sample 4, the sample with the highest oxygen content in the overall composition. At 1825° C, however, almost all samples were dense, with the exception of samples 2, 3 and 5 at higher cerium contents (see Fig. 3b). For pure CeO_2 additions the relative densities of samples 3 and 5 were about 99% and 96% theoretical, respectively. It can be noted that these overall compositions are furthest away from the liquid-phase region in the cerium–sialon phase diagram, and that sample 5 has the highest nitrogen content of all samples.

Examination with an optical microscope of the porosity level of the dense samples sintered at 1825° C showed that only microporosity was present and varied in a non-systematic way between 0 and about 1 vol % pores, the most typical value being about 0.6 vol %. The only sample with no measureable porosity was sample 4 with pure Y_2O_3 additions, but even this composition had about 0.5 vol % pores at pure CeO_2 additions.

3.2. X-ray diffraction analysis

The results of the X-ray diffraction analysis are summarized in Table I. No significant differences were observed between the phases present at the two different temperatures. It could be seen that samples 1 and 4, as expected, contained only β sialon as the major crystalline phase. The other samples, in the case of pure Y_2O_3 additions, were mixed α–β sialon materials, but with increasing substitution of cerium for yttrium the amount of α sialon declined to zero.

In samples 2, 3 and 5 some weak or very weak reflections due to other phases could be seen in addition to those from the sialon phases for higher cerium contents. In some instances a positive identification was impossible, but in the samples with pure CeO_2 additions the additional phases could be identified as cerium nitrogen α-wollastonite ($CeSiO_2N$) and as cerium silicon oxynitride ($Ce_2Si_6O_3N_8$). The calculated z value for the β sialon phase $Si_{6-z}Al_zO_zN_{8-z}$ increases slightly with increasing overall aluminium content of the yttrium containing samples, as expected from the position in the phase diagram, i.e. in the order samples 1, 2 and 3. A second trend for the z values is that it remains unaffected for the β sialon materials (1 and 4) by increasing replacement of Y_2O_3 by CeO_2, but for the mixed α–β sialon ceramics a slight decrease in z is observed. The unit cell dimensions of the α sialon phase remain pratically the same

TABLE I The results of the X-ray diffraction analysis of the sample series pressureless sintered at 1825° C for 2 h

Sample	Y_2O_3/CeO_2 ratio	Observed phases	$\alpha/(\alpha+\beta)$ sialon ratio	z value (β sialon)
1	100/0	β sialon	0	0.49
	75/25	β sialon	0	0.42
	50/50	β sialon	0	0.48
	25/75	β sialon	0	0.44
	0/100	β sialon	0	0.46
2	100/0	β sialon, α sialon	0.29	0.63
	75/25	β sialon, α sialon	0.22	0.64
	50/50	β sialon, α sialon*	0.12	0.63
	25/75	β sialon, α sialon (traces)*	0.01	0.59
	0/100	β sialon, $CeSiO_2N$ (weak)*	0	0.43
3	100/0	β sialon, α sialon	0.39	0.67
	75/25	β sialon, α sialon	0.28	0.69
	50/50	β sialon, α sialon*	0.16	0.67
	25/75	β sialon, α sialon (weak)*	0.03	0.62
	0/100	β sialon, $CeSiO_2N$ (weak)*	0	0.55
4	100/0	β sialon	0	0.62
	75/25	β sialon	0	0.65
	50/50	β sialon	0	0.59
	25/75	β sialon	0	0.62
	0/100	β sialon	0	0.67
5	100/0	β sialon, α sialon	0.58	0.60
	75/25	β sialon, α sialon	0.47	0.55
	50/50	β sialon, α sialon	0.33	0.51
	25/75	β sialon, α sialon*	0.17	0.47
	0/100	β sialon, $Ce_2Si_6O_3N_8$ (weak)	0	0.39

*One to five weak or very weak unidentified lines present.

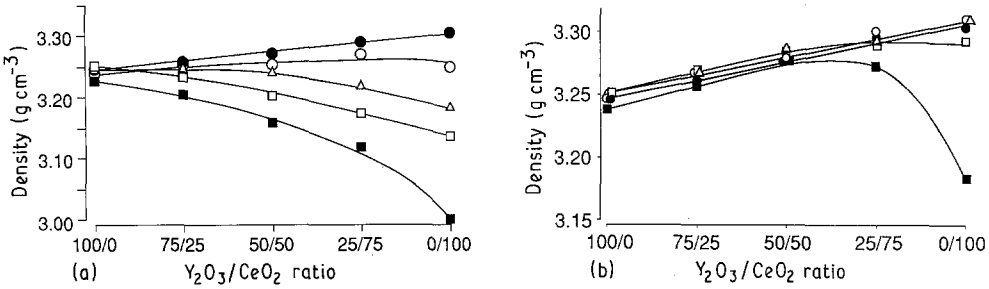

Figure 3. Density variations of the sialon materials with different Y_2O_3/CeO_2 additions, made by pressureless sintering at 1775 and 1825° C, illustrated in (a) and (b), respectively. Samples: (○) 1, (△) 2, (□) 3, (●) 4, (■) 5.

in all specimens where this phase is observed, being $a = 0.7802$ nm and $c = 0.5683$ nm for the hexagonal cell. The observed values vary randomly within ± 0.0004 nm.

3.3. Microstructural studies

Typical changes in the microstructure on replacing yttrium by cerium are illustrated for a β sialon ceramic (4) and an α–β sialon ceramic (3) in Figs 4a to c and d to f, respectively. In the case of β sialon ceramics the intergranular phase of white contrast contains all the added yttrium or cerium ions. This was found by energy dispersive X-ray spectrometry (EDS) analysis in the SEM and by the analysis with electron microprobe, as no yttrium or cerium signals were obtained from the β sialon grains. In the mixed α–β sialon ceramics most of the added yttrium and practically all the cerium was also found in the intergranular phase. It should, however, be stressed that the content of yttrium and cerium varied somewhat from one glassy phase pocket to another in the same material.

A slight increase in the amount of intergranular phase could be seen in the β sialon sample 4 when Y_2O_3 was replaced by CeO_2. A similar slight increase of the intergranular content was also observed in the α–β sialon material of sample 3.

The EDS analysis of α sialon grains clearly showed that yttrium had entered into the structure, but it could not be ascertained by this technique whether or not any cerium was present. A more detailed analysis was therefore performed by electron microprobe on the α sialon phase present in the $Y_2O_3/CeO_2 = 75/25$ specimen of composition 2. An analysis of a $50 \times 50\,\mu m^2$ area of the specimen was used as a calibration of the yttrium and cerium signals. It was found that the major element entering the α sialon was yttrium, but a small peak, clearly above the background noise, showed that a small amount of cerium corresponding to about 0.5 wt %, was also present in the α sialon.

The β sialon grains have a typical elongated shape and a hexagonal cross-section, whereas the α sialon grains are more plate-like. The materials with pure Y_2O_3 additions in general had a somewhat coarser grain than the CeO_2 doped materials, and the addition of the mixture $Y_2O_3/CeO_2 = 50/50$ seemed to form the smallest grains, whereas a further increase in the cerium content towards pure CeO_2 additions caused the grains to grow slightly larger.

A visual comparison of scanning electron micrographs showed that compositions 2 and 4 had the largest proportion of elongated β sialon grains of high "aspect ratio", i.e. high length to diameter ratio. This was especially pronounced for the mixed Y_2O_3/CeO_2 additions, and the aspect ratios for a 50/50 addition were in the range 3 to 11 and 5 to 11 for compositions 2 and 4, respectively.

3.4. Mechanical properties

The mechanical properties have only been measured on the samples sintered at 1825° C, as most of these samples have a theoretical density above 99% and are likely to give representative results. A summary of the observed hardness and fracture toughness values is shown in Fig. 5. For the samples with a density below 99%, the lines have been drawn dashed in the figure to emphasize that these values are less reliable.

The sintered sialon ceramics with pure Y_2O_3 additions could be divided into two different groups depending on the presence or absence of an α sialon phase, i.e. into β sialon and mixed α–β sialon ceramics, and this is also reflected in the mechanical properties. This is easily seen in Fig. 5, where the hardness of the α–β sialon materials with pure Y_2O_3 additions increases as a function of the α sialon content, i.e. in the order samples 2, 3 and 5. The β sialon materials 1 and 4 are significantly softer. The α sialon content, however, decreases with increasing CeO_2 content, and this is clearly reflected in a corresponding decrease in the hardness. Similarly the fracture toughness of the β sialon ceramics is usually higher than that of the α–β sialon ceramics with Y_2O_3 additions only, which is seen in Fig. 5b. The replacement of yttrium with cerium gives an increase in the fracture toughness for most of the samples. In fact, for the β sialon sample 4 the increase from 5 to 6 MPa $m^{1/2}$ is significant and combined with retained hardness. The mixed α–β sialon sample 2 also shows an increase in the fracture toughness up to Y_2O_3/CeO_2 ratios of 50/50. The apparent increase in toughness for the composition 5 at higher degrees of CeO_2 doping, indicated by the dashed line in the figure, has been measured on materials which are not fully dense and is believed to reflect the increase in the porosity level.

4. Discussion

The measured density (g cm^{-3}) for a sialon material is affected by several different factors in addition to the porosity level, and a complementary study by optical microscopy or SEM on carefully polished cross-sections of the samples is needed. It is, however, important that the final polishing step is very gentle to avoid tearing out grains or iron silicides possibly

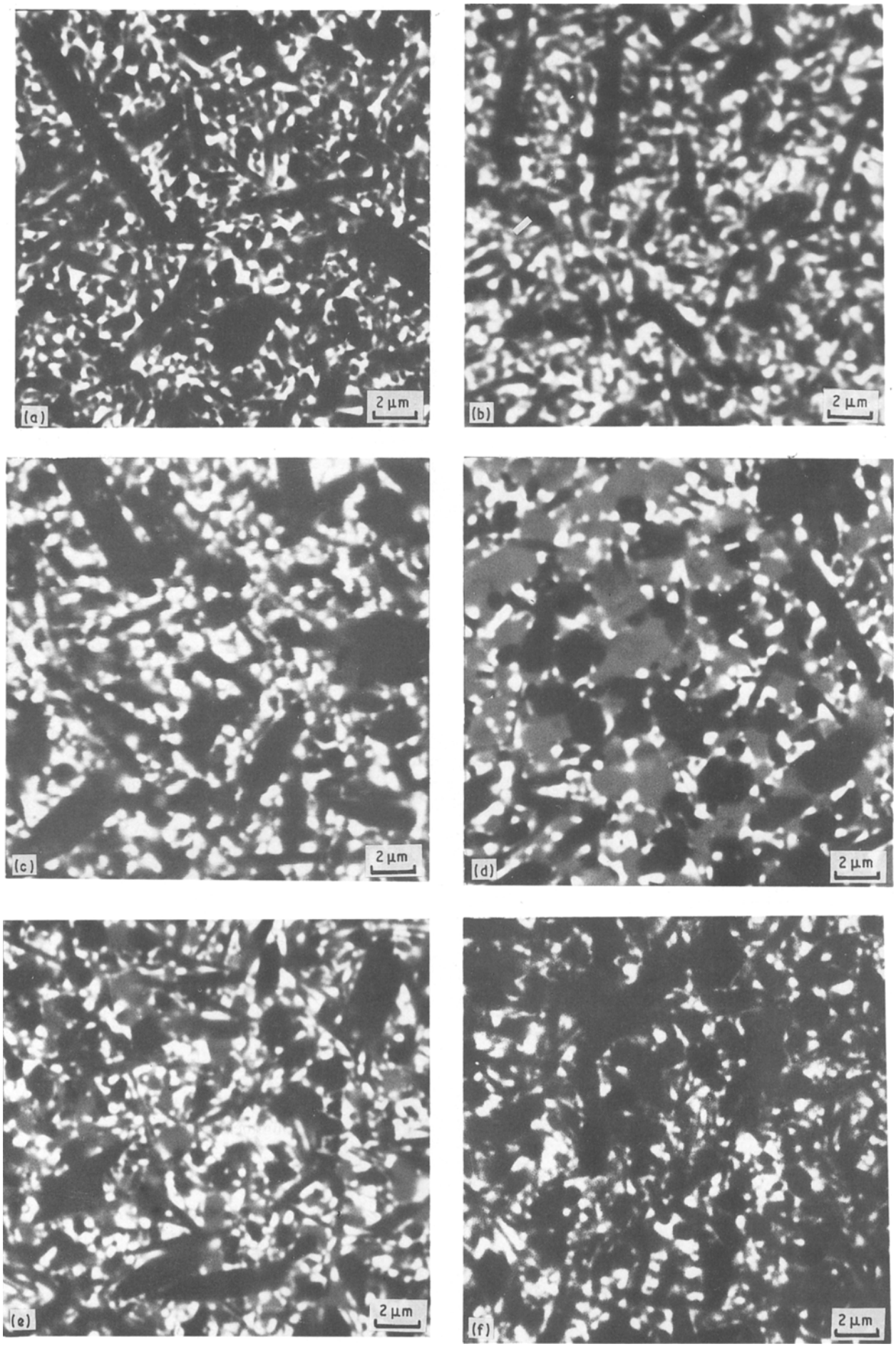

Figure 4. Scanning electron micrographs registered by back-scattered electrons (15 kV, *z*-contrast) to illustrate the microstructure of a β sialon sample (4) sintered at 1825° C for pure (a) Y_2O_3, (b) 50/50 and (c) pure CeO_2 additions. Similar micrographs of an α–β sialon ceramic (3) are found in (d), (e) and (f). The intergranular phase has a white contrast, the β sialon grains are dark, and in (d) and (e) the α sialon grains appear with grey contrast, as this phase contains some yttrium.

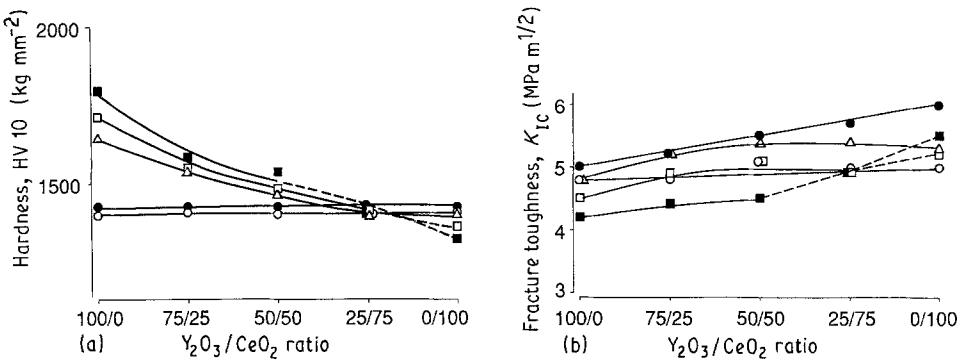

Figure 5. The Vickers hardness with a 98 N load (HV 10) and the indentation fracture toughness (K_{IC}) of samples made by pressureless sintering at 1825° C, cf. text. Samples: (○) 1, (△) 2, (□) 3, (●) 4, (■) 5.

present, which would give a false apparent increase in porosity. The other factors affecting the density are, of course, the relative amounts and densities of the different phases present. Thus, typical density values for the phases found in these samples are 3.18, 3.28 and 4 g cm^{-3} for the β sialon, α sialon and glassy phase, respectively.

The results of the present study show that at 1775° C the only sample with good densification was sample 4, the composition with the highest oxygen content of the prepared samples and with a fair amount of aluminium, which lowers the viscosity of the liquid formed at the sintering temperature.

At 1825° C the densification of more nitrogen-rich compositions is possible, but still sample 5 with the highest nitrogen content did not consolidate at higher cerium dopings. The sintering temperature cannot be raised further with the BN powder bed technique used in this study, because the samples will then suffer increasing weight losses. At 1825° C the weight loss during 2 h sintering is 2 to 3 wt % at most, but a further rise in sintering temperature to 1850° C will result in a dramatic increase in weight loss, caused by an accelerating decomposition of the silicon nitride. One way to overcome this problem might be sintering in pressurized nitrogen gas.

The very weak unidentified peaks found by X-ray diffraction are probably due to other cerium silicon oxynitride or silicate phases, cf. Fig. 2. However, it cannot be said whether these phases or the two identified phases, $CeSiO_2N$ and $Ce_2Si_6O_3N_8$, are formed at the sintering temperature or during cooling either by crystallization from the melt or by devitrification of the glassy phase. Previous experience from the pure yttrium-sialon system has shown that if the cooling rate is slow enough, yttrium aluminium garnet (YAG) can be crystallized from the melt at about 1450° C or the so-called b-phase (α-wollastonite type, Y_2SiAlO_5N) can form by devitrification of the glassy phase at about 1100° C.

The small shift in the z value for the β sialon phase, observed for the α-β sialon ceramics with increasing replacement of Y_2O_3 by CeO_2, is believed to be caused by changes in the liquid composition at the sintering temperature by the change in the α to β sialon phase ratio.

In none of the compositions did α sialon form during pressureless sintering with pure CeO_2 additions. This implies that all CeO_2 during the heating to the sintering temperature has been converted to Ce_2O_3. The ion size of Ce^{4+} in six-coordination is 0.080 nm, compared with 0.089 nm for Y^{3+}, and the Ce^{4+} ion is therefore small enough to enter the α phase structure, thereby stabilizing the α sialon. The ion size of Ce^{3+}, however, is 0.103 nm which is larger than the size of Nd^{3+}, 0.100 nm, which is the largest ion found to stabilize the α sialon phase. The behaviour of Ce^{3+} is thus similar to that of La^{3+} (0.106 nm), which is found not to stabilize the α sialon [19, 20].

One interesting observation made in this study is that a very small amount of cerium seems to have entered the α sialon grains together with yttrium, despite the fact that with pure ceria additions no indications were found by X-ray diffraction that any α sialon phase was formed. We believe, however, that there might be a synergetic effect of the simultaneous presence of both ions.

In the present preparations, cerium is added as CeO_2, i.e. as Ce^{4+}, but as this oxidation state is not stable at very high temperatures, a red–ox process will convert Ce^{4+} to Ce^{3+}. It is not known exactly at which temperature this will take place during the present sintering conditions, as the samples are heated continuously up to the sintering temperature, and the transformation may be extended over some range of temperature and time. It might well be that the recrystallization of α sialon, stabilized mainly by yttrium, might have started while some Ce^{4+} is still present in the melt, and some of this cerium may therefore also enter into the α sialon phase. To confirm this speculation, studies have been started to prepare cerium-containing sialon ceramics at high pressure (HIP-technique) and at lower temperatures. Both these factors are expected to keep the Ce^{4+} ion more stable.

In this context it can be mentioned that a pressureless-sintered sialon ceramic with mixed Y_2O_3/CeO_2 additions has been studied previously by high resolution transmission electron microscopy [21]. A number of new defect types were found in the α sialon crystals, which implies a special tendency of the presence of cerium to initiate defects in the lattice. The author suggested that the defects might be caused by inclusion in the structure of trapped Ce^{3+}, formed by reduction of Ce^{4+} ions that was incorporated during some stage of the annealing process.

It is generally believed that the eutectic temperature, composition and viscosity of the liquid at the sintering temperature will affect the size and shape of the β sialon grains by somewhat different nucleation and/or growth mechanisms. In this study we have observed a change in grain size with different degrees of cerium doping, as well as some changes in grain shape. The presence of elongated β sialon grains with a high aspect ratio favours higher fracture toughness of the materials. This fits in well with our findings, as compositions 2 and 4 were found by SEM to have β sialon grains of high aspect ratio and these two compositional series were found to have the highest toughness values, especially for mixed Y_2O_3/CeO_2 additions.

The hardness of a material will be influenced by the porosity level, the relative amount and hardness of the constituent phases, grain size etc. In these materials the hardness has been found to be strongly affected by the α sialon content, as this phase is harder (HV 10 $\sim 2000\,kg\,mm^{-2}$) than the β sialon phase (HV 10 $\sim 1700\,kg\,mm^{-2}$) or the glassy phase (HV 10 $\sim 1000\,kg\,mm^{-2}$). A slight overall increase of the hardness could be seen for the β sialon materials with cerium replacing yttrium, probably depending on an increased hardness of the glassy phase.

5. Conclusions

1. The less expensive CeO_2 oxide can successfully replace Y_2O_3 as an additive in pressureless sintering of dense sialon ceramics at a temperature of 1825° C and the added amount of CeO_2 does not need to exceed 9.3 wt %.

2. The indentation fracture toughness K_{IC} of CeO_2-doped sialons is of the same magnitude as for the pure Y_2O_3 additions, or higher.

3. In one of the β sialon materials the K_{IC} value increased from 5 to 6 MPa $m^{1/2}$, and the hardness from about 1400 to 1500 $kg\,mm^{-2}$, when Y_2O_3 was totally replaced by CeO_2.

4. At high temperatures, the Ce^{3+} ion present does not stabilize the α sialon phase and, consequently, in the mixed α–β sialon ceramics the α phase content and the hardness decreased with increasing cerium doping.

Acknowledgements

AB Sandvik Hard Materials is thanked for permission to publish the results presented in this article. The work was financed in part by the Swedish Board for Technical Development.

References

1. E. GLENNY and T. A. TAYLOR, *Powder Metall.* **1–2** (1958) 189.
2. F. THUMMLER, in "Keramische Komponenten für Fahrzeug-Gasturbinen", edited by W. Bunk and M. Böhmer (Springer Verlag, Berlin, 1978) p. 253.
3. K. H. JACK, *J. Mater. Sci.* **11** (1976) 1135.
4. *Idem, Sci. Ceram.* **11** (1981) 125.
5. M. BURSTRÖM, J. ADLERBORN and L. HERMANSSON, in "Proceedings Hot Isostatic Pressing", edited by T. Garvare (Centek, Luleå, Sweden, 1988) p. 383.
6. T. EKSTRÖM, *Mater. Sci. Forum* **34–36** (1988) 605.
7. D. P. THOMPSON, in "Tailoring Multiphase and Composite Ceramics", edited by R. E. Tressler, G. L. Messing, C. G. Pantano and R. E. Newham (Plenum, New York, 1986) p. 79.
8. I. C. HUSEBY and G. PETZOW, *Powder Met. Int.* **6** (1974) 17.
9. T.-I. MAH, K. S. MAZDIYASNI and R. RUH, *J. Amer. Ceram. Soc.* **72** (1979) 12.
10. *Idem, Amer. Ceram. Soc. Bull.* **58** (1979) 840.
11. W. A. SANDERS and D. M. MIESKOWSKI, *ibid.* **64** (1985) 304.
12. E. TANI, S. UMEBAYASHI, K. KISHI, K. KOBAYASHI and M. NISHIJIMA. *ibid.* **65** (1986) 1311.
13. N. HIROSAKI, A. OKADA and K. MATOBA, *J. Amer. Ceram. Soc.* **71** (1988) C-144.
14. F. F. LANGE, *Amer. Ceram. Soc. Bull.* **59** (1980) 239.
15. A. ARIAS, *J. Mater. Sci.* **16** (1981) 787.
16. G. R. ANSTIS, P. CHANTIKUL, B. R. LAWN and D. P. MARSHALL, *J. Amer. Ceram. Soc.* **64** (1981) 533.
17. T. EKSTRÖM, P. O. KÄLL, M. NYGREN and P. O. OLSSON, *J. Mater. Sci.* **24** (1989) 1853.
18. P. O. KÄLL, *Chem. Scripta* **28** (1988) 439.
19. T. EKSTRÖM and P. O. OLSSON, *J. Mater. Sci. Lett.* **8** (1989) 1067.
20. P. O. OLSSON and T. EKSTRÖM, *J. Mater. Sci.* **25** (1990) 1824.
21. P. O. OLSSON, *J. Mater. Sci.* **24** (1989) 3878.

Received 27 June
and accepted 1 December 1989